NASA TECHNICAL NOTE

NASA TN D-8260

NASA TN D-8260

CASE FILE COPY

A DESIGN APPROACH AND SELECTED WIND-TUNNEL RESULTS AT HIGH SUBSONIC SPEEDS FOR WING-TIP MOUNTED WINGLETS

Richard T. Whitcomb

Langley Research Center
Hampton, Va. 23665

NATIONAL AERONAUTICS AND SPACE ADMINISTRATION • WASHINGTON, D. C. • JULY 1976

1. Report No. NASA TN D-8260	2. Government Accession No.	3. Recipient's Catalog No.
4. Title and Subtitle A DESIGN APPROACH AND SELECTED WIND-TUNNEL RESULTS AT HIGH SUBSONIC SPEEDS FOR WING-TIP MOUNTED WINGLETS		5. Report Date July 1976
		6. Performing Organization Code
7. Author(s) Richard T. Whitcomb		8. Performing Organization Report No. L-10908
9. Performing Organization Name and Address NASA Langley Research Center Hampton, Va. 23665		10. Work Unit No. 505-11-16-08
		11. Contract or Grant No.
12. Sponsoring Agency Name and Address National Aeronautics and Space Administration Washington, D.C. 20546		13. Type of Report and Period Covered Technical Note
		14. Sponsoring Agency Code

15. Supplementary Notes

16. Abstract

    Winglets, which are small, nearly vertical, winglike surfaces, substantially reduce drag coefficients at lifting conditions. The primary winglet surfaces are rearward above the wing tips; secondary surfaces are forward below the wing tips. This report presents a discussion of the considerations involved in the design of the winglets; measured effects of these surfaces on the aerodynamic forces, moments, and loads for a representative first-generation, narrow-body jet transport wing; and a comparison of these effects with those for a wing-tip extension which results in approximately the same increase in bending moment at the wing-fuselage juncture as did the addition of the winglets.

17. Key Words (Suggested by Author(s)) Nonplanar lifting systems Aerodynamic drag reduction Induced drag	18. Distribution Statement Unclassified — Unlimited Subject Category 02		
19. Security Classif. (of this report) Unclassified	20. Security Classif. (of this page) Unclassified	21. No. of Pages 30	22. Price* $3.75

A DESIGN APPROACH AND SELECTED WIND-TUNNEL RESULTS AT
HIGH SUBSONIC SPEEDS FOR WING-TIP MOUNTED WINGLETS

Richard T. Whitcomb
Langley Research Center

SUMMARY

Winglets, which are small, nearly vertical, winglike surfaces mounted at the tips of a wing, are intended to provide, for lifting conditions and subsonic Mach numbers, reductions in drag coefficient greater than those achieved by a simple wing-tip extension with the same structural weight penalty. The primary surfaces are located rearward above the tips. Smaller secondary surfaces may be placed forward below the tips. This paper includes a discussion of the considerations involved in the design of such surfaces; the measured effects of these surfaces on the aerodynamic forces, moments, and loads near the design conditions for a representative first-generation, narrow-body jet transport wing; and a comparison of these effects with those for a wing-tip extension which results in approximately the same increase in bending moment at the wing-fuselage juncture as did the addition of the winglets. The experiments were conducted in the Langley 8-foot transonic pressure tunnel.

For the configuration investigated the winglets reduce the induced drag by about 20 percent with a resulting increase in wing lift-drag ratio of roughly 9 percent for the design Mach number of 0.78 and near the design lift coefficient. This improvement in lift-drag ratio is more than twice as great as that achieved with the comparable wing-tip extension. Also, the negative increments in pitching-moment coefficients associated with the addition of the winglets are less than those produced by the wing-tip extension. The experimental results also indicate that the increase in overall performance improvement provided by the winglets in comparison with that for a wing-tip extension is significantly dependent on the angles of incidence of the upper winglet.

INTRODUCTION

It has been recognized for many years that a nonplanar lifting system should have less induced drag than a planar wing. As early as 1897 a patent was obtained by Lanchester for vertical surfaces at the wing tips. Since that time a number of theoretical analyses have indicated the significant improvements possible with nonplanar systems including vertical surfaces at the tip. (See refs. 1 to 3, for example.) On the basis of

these encouraging theoretical studies, a number of experimental investigations of various end plates at the wing tips have been made. Usually these surfaces have reduced the drag at very high lift coefficients but have resulted, at best, in only slight reductions in drag near cruise lift coefficients. Near cruise conditions the viscous drag increments associated with the end plates were nearly as great as the reductions in induced drag.

An analysis of the effect of vertical surfaces at the tip on overall airplane performance must include consideration of the effect of such surfaces on the structural weight. Loads on the vertical surfaces and the increased loads on the outboard region of the wing associated with adding these surfaces increase the bending moments imposed on the wing structure. The greater bending moments, of course, require a heavier wing structure. Aircraft designers have found that for the same structural weight penalty associated with adding end plates, a significantly greater improvement in drag could be achieved by merely extending the wing tip. As a result, no aircraft designs have incorporated such surfaces for the sole purpose of reducing drag. However, vertical surfaces have been placed near the tips of some sweptback and delta wings to provide directional stability. The objective of the work described herein was to develop nearly vertical, tip mounted surfaces which would provide, near cruise conditions, substantially greater reductions in drag coefficient than those resulting from tip extensions with the same added bending moments imposed on the wing structure.

The factor that most previous experimental investigators have overlooked is that to be fully effective the vertical surface at the tip must efficiently produce significant side forces. These side forces are required to reduce the lift-induced inflow above the wing tip or the outflow below the tip. Obviously, a low-aspect-ratio flat end plate as generally tested previously is not an efficient lifting surface. To achieve the stated objective of the present work, the nearly vertical surfaces placed at the tip for the purpose of reducing drag due to lift have been designed to produce significant side forces, even at supercritical conditions, according to the well-established principles for designing efficient wings; hence the name winglets. Flow surveys behind the tip of a wing with and without winglets, presented in reference 4, indicate that the basic physical effect of the winglets, which leads to drag reduction, is a vertical diffusion of the tip vortex flow at least just downstream of the tip. The large inward components of the vortex flow near the center of the vortex are substantially reduced while the small inward components in the region above the tip of the winglet are increased slightly. Thus these surfaces could be called vortex diffusers.

The initial development investigations of wing-tip mounted winglets were conducted at subsonic speeds on a representative second-generation, wide-body jet transport wing in the Langley 8-foot transonic pressure tunnel during 1974. The results of that investigation are discussed in general terms in reference 5. Complete results for the final configuration of that investigation are presented in reference 4. Recently, improved winglets have been investigated on a representative first-generation, narrow-body jet transport wing for

a wider range of flight conditions than that of reference 4. This report describes the approach used in the design of the winglets, presents selected results from the more recent wind-tunnel investigation, and compares the results with the design objective.

SYMBOLS

The longitudinal aerodynamic characteristics presented in this report are referred to the stability axis system. Force and moment data have been reduced to coefficient form on the basis of the exposed area of the basic wing, except for the normal-force coefficients for the winglets. The reference for pitching moments is the quarter-chord of the mean aerodynamic chord of the wing. All dimensional values are given in both the International System of Units (SI) and U.S. Customary Units (ref. 6). All measurements and calculations were made in U.S. Customary Units.

Coefficients and symbols used herein are defined as follows:

b' exposed semispan of wing with basic tip, 124.26 cm (48.92 in.)

$\Delta b'$ incremental increase in exposed wing semispan, 0.38h, 7.62 cm (3.00 in.)

c local chord, cm (in.)

$\bar{c}$ mean aerodynamic chord of exposed basic wing, 39.98 cm (15.74 in.)

c_{av} average chord of exposed basic wing, $\frac{S}{b'}$, 37.41 cm (14.73 in.)

c_n section normal-force coefficient obtained from integrated pressure measurements

c_t tip chord of basic wing

C_b bending-moment coefficient of wing at wing-fuselage juncture, $\dfrac{\text{Bending moment}}{q_\infty S b'}$

C_D drag coefficient, $\dfrac{\text{Drag}}{q_\infty S}$

C_L lift coefficient, $\dfrac{\text{Lift}}{q_\infty S}$

ΔC_L incremental lift coefficient at constant drag coefficient,

$$\left(C_L\right)_{\substack{\text{with winglets or} \\ \text{tip extension}}} - \left(C_L\right)_{\text{basic wing}}$$

C_m pitching-moment coefficient about moment reference center, $\dfrac{\text{Pitching moment}}{q_\infty S\bar{c}}$

C_N normal-force coefficient obtained by integrating span load distribution, based on winglet area

C_p pressure coefficient, $\dfrac{p_l - p_\infty}{q_\infty}$

$C_{p,\text{sonic}}$ pressure coefficient corresponding to local speed of sound

h   span of upper winglet from chord plane of wing tip (see fig. 3), 20.32 cm (8.00 in.)

i   incidence of winglet measured from free-stream direction, positive with leading edge inward for upper winglet, with leading edge outward for lower winglet (see fig. 3), deg

M_∞ free-stream Mach number

p_l local static pressure, N/m^2 (psf)

p_∞ free-stream static pressure, N/m^2 (psf)

q_∞ free-stream dynamic pressure, N/m^2 (psf)

S   area of exposed basic wing, 0.4649 m^2 (5.0034 ft^2)

x   chordwise distance from leading edge, positive aft, cm (in.)

y   spanwise distance from wing-fuselage juncture, positive outboard, cm (in.)

z   vertical coordinate of airfoil, positive upward, cm (in.)

4

z'   distance along winglet span from chord plane of wing, cm   (in.)

α angle of attack, deg

DESIGN CONSIDERATIONS

Methodology

The theoretical calculations of references 3 and 7 provide an indication of the span load distributions required on the wing and vertical surfaces at the tip to obtain the optimum induced drag in subcritical flow. However, they do not describe how the configuration should be shaped to obtain these load distributions or how it should be designed to achieve the maximum improvement in overall performance. The tip mounted winglets of the present investigation were developed with the available theoretical calculations, physical flow considerations, and extensive exploratory experiments. Consideration has been given to the effect of adding the winglets on the structural weight and the high-lift off-design performance as well as to the drag reduction at design conditions. Because of the limitations of the methods used, the winglets of this investigation are undoubtedly not optimum.

Since the development of the design approach described herein, several new theoretical lifting surface methods for analyzing and optimizing nonplanar lifting systems for subcritical flows have been developed. Among them are references 8 and 9. These methods should greatly aid in future aerodynamic designs of more nearly optimum winglets. Calculations based on the method of reference 9 have already been used to verify a number of the assumptions made in the design procedure presented herein. They have also indicated several areas where the design might be improved. Some of the applications of this theory are described subsequently in this report.

Upper Winglet

Arrangement.- The primary component of the winglet configuration (figs. 1, 2, and 3) is a nearly vertical surface mounted rearward above the wing tip. The upper winglet is placed rearward so that the increased velocities over the inner surface of the winglet are not superimposed on the high velocities over the forward region of the wing upper surface. Thus adverse flow interference effects at supercritical design conditions are reduced. The results of exploratory investigations suggest that to minimize adverse interference effects at supercritical conditions, the leading edge of the root of the winglet should probably not be significantly ahead of the upper-surface crest of the wing-tip section. Conversely, if the leading edge of the upper winglet is moved aft of this crest, attachment of this surface to the wing becomes a greater problem since the structural box

5

for the winglet moves aft of the usual rear spar location for the wing. Also, analyses and exploratory experiments indicate that the shorter winglet root chord caused by moving the leading edge aft of the wing section crest results in a perceptible loss of winglet effectiveness. Therefore the leading edge of the winglet has been placed near the crest for cruise conditions. Results of exploratory experiments also indicate that the greatest winglet effectiveness is achieved with the trailing edge of the winglet near the trailing edge of the wing.

Loads.- The theories of references 3, 7, and 9 indicate that to achieve the reductions in induced drag theoretically predicted for wing-tip mounted vertical surfaces requires not only substantial inward normal loads on these surfaces but also significant increases in the upward loads on the outboard region of the wing. Exploratory experiments made both during the investigation of reference 4 and during the present investigation indicate that the greatest measured reductions in drag due to adding the upper winglet are achieved with normal loads on the winglet, and associated added loads on the outboard region of the wing, substantially less than those indicated as optimum by the theories of references 3, 7, and 9. These differences are probably due primarily to viscous effects not included in theory. Calculations based on reference 9 indicate that reducing these loads from the theoretical optimum values to the measured values decreases the effectiveness of the winglets only slightly (induced drag increases slightly). This effect is probably more than offset by a reduction in viscous drag for both the winglet and the wing resulting from lower induced velocities on these surfaces at the lower load condition. Further, with such reduced loads the added bending moments imposed on the wing and the resulting structural weight increase are less than those associated with the theoretically optimum loads.

The theories of references 3 and 7 indicate that the optimum span load distributions for the winglet are characterized by relatively high loads near the winglet root in comparison with the optimum elliptical load distribution for planar wings.

Height.- The available theories (ref. 3, for example) indicate that the reduction in induced drag associated with tip mounted vertical surfaces increases slightly less than linearly with increase in height. However, the theories indicate that the normal loads on such surfaces and the loads on the outboard region of the wing required for the calculated induced drag reduction also increase with an increase in winglet height. These greater loads, together with a greater moment arm of the loads on the winglet associated with increased height, of course, increase the bending moments in the wing with a resulting weight penalty. Therefore, the optimum height must be a compromise between aerodynamic and structural weight considerations.

Further, the required normal-force coefficients for the winglet increase with an increase in winglet height. For excessive winglet heights the required normal-force coefficients would lead to substantial boundary-layer separation particularly for high-lift

6

off-design conditions. For the most satisfactory results the required normal-force coefficients for the winglet should probably be limited to values of the same order of magnitude as the lift coefficients of the wing.

The height of the winglet of the investigation described herein was selected arbitrarily on the basis of very limited exploratory experiments and analyses. A precise determination of the most satisfactory height must await more definite information on the structural weight penalties associated with adding winglets.

Planform.- As for wings, the winglet should have the highest aerodynamic efficiency when it is tapered so that the normal-force coefficient is approximately constant along the span of the winglet. To achieve this situation for the desired span load distribution requires substantial taper. For satisfactory winglet effectiveness at supercritical design conditions, the effective sweep of these surfaces should be approximately the same as that of the wing.

Airfoil section.- The winglet airfoil should be shaped to meet two important basic requirements. First, it should efficiently provide the desired inward normal-force coefficients for the design wing lift coefficient and Mach number. For supercritical design conditions, this objective is achieved with an airfoil shaped to avoid a strong wave on the surface and to minimize the added induced velocities on the outboard region of the wing upper surface associated with the presence of the winglet. Secondly, the airfoil should be shaped so that the onset of significant boundary-layer separation on the winglet surface is delayed to the conditions for which such separation occurs on the wing. This latter objective should be achieved even for low-speed high-lift conditions with the stall control devices extended on the wing.

These objectives are probably accomplished most effectively with an airfoil similar to the NASA general aviation airfoil described in reference 10 with a design camber significantly greater than that for the wing. Experiments and theoretical analyses have indicated that such an airfoil provides superior low-speed high-lift characteristics and satisfactory supercritical characteristics. Also, to accomplish the high-speed objectives most effectively, the maximum ratio of airfoil thickness to chord should be as low as possible without causing a severe weight penalty or significantly degrading the low-speed stall characteristics. Preliminary structural and aerodynamic studies suggest that the most satisfactory thickness ratio may be about 8 percent.

Incidence and twist.- The upper winglet is generally toed out and thus has negative geometric incidence, since the effective inflow angles are greater than the winglet angles of attack required to achieve the desired normal-force coefficient for design conditions. With the large amount of camber required in the winglet, this negative incidence can be substantial. Because the available theories do not as yet incorporate effects of viscosity,

7

thickness, and supercritical flow, the most satisfactory incidence must at present be determined by a systematic experimental investigation of various incidence angles.

To obtain the desired span load distribution on a swept upper winglet in an undistorted flow field would require substantial twist. However, the decrease in inflow with increase in winglet height above the wing approximately provides the desired aerodynamic twist. Thus, no geometric twist is usually required for this surface.

Cant or dihedral.- A study, based on theoretical calculations made by J. L. Lundry using the method of reference 7, of the trade-offs between induced drag reduction, skin friction, and wing bending moments indicates that the optimum practical winglet configuration should have a small amount of outward cant as shown in figure 1. Outward cant also reduces the flow interference at the root of the upper winglet at supercritical conditions.

Lower Winglet

Rationale.- Theoretically, a nearly vertical surface below the wing tip is as effective as one of the same height above the tip. However a lower winglet usually must be shorter than the optimum height because of ground clearance problems. The theoretical calculations of reference 3 indicate that a lower winglet of practical vertical height, in combination with a larger upper winglet, produces relatively small additional reductions in induced drag. However, experiments indicate that even such a shortened surface may improve overall winglet effectiveness, particularly at both high lift coefficients and supercritical conditions. The presence of a lower winglet lessens both the theoretically desired (refs. 3 and 7) and actually measured optimum induced velocities on the upper winglet, with a resulting decrease in boundary-layer separation on the winglet inner surface.

Forward placement of the lower winglet maximizes the reduction in the usual maximum induced velocity on the forward region of the inner surface of the upper winglet at high wing lift coefficients. This effect is roughly similar to that of a slat near the leading edge of a wing; in both cases the local angle of flow at the leading edge is reduced. It is conjectured that this favorable effect is nearly optimum when the trailing edge of the root of the lower winglet coincides streamwise with the leading edge of the upper winglet.

Configuration.- Because of the pronounced interactions of the high induced velocities on the forward portion of the wing with those on the lower winglet, the definition of the most satisfactory configuration of the lower winglet for the complete range of flight conditions is far from complete. However it is known that, as for the upper winglet, the lower winglet requires substantial camber (upper surface outward) and toe-in. Preliminary analyses, substantiated by calculations based on reference 9, also suggest that, in contrast to the upper winglet, the lower winglet should probably be twisted with washout.

8

An analysis based on the theoretical results of reference 3 suggests that outward cant of the lower winglet would increase the favorable effect of this surface on the flow over the upper winglet. Therefore substantial outward cant was incorporated in this surface for the configuration of reference 4 and that of the present report. However, a more recent analysis, using the method of reference 9, indicates that the most satisfactory overall performance is probably achieved with little or no cant in this surface.

EXPERIMENTS

Apparatus and Procedures

Test facility.- This investigation was conducted in the Langley 8-foot transonic pressure tunnel, a continuous single-return tunnel with a slotted rectangular test section. The longitudinal slots in the floor and ceiling of the test section reduce tunnel wall interference and allow relatively large models to be tested through the subsonic speed range. Mach number, stagnation pressure, temperature, and dewpoint are independently variable. A more detailed description of the tunnel is found in reference 11.

Model description.- In an effort to obtain the highest possible winglet Reynolds number and sufficient winglet size to install surface-pressure measurement tubes, a semispan model was utilized. Photographs of the model in the wind tunnel are shown in figure 1. Drawings of the model configurations are shown in figures 2 and 3. The basic fuselage, wing, and nacelles approximate those of a representative first-generation, narrow-body jet transport. The fuselage was not attached to the balance but did rotate with the wing through the angle-of-attack range. The midsection covered the balance and had a slot through which the wing protruded. The model wing stiffness was designed so that the nondimensional tip bending deflection was approximately the same as that for the actual airplane at design conditions of $M_\infty = 0.78$ and $C_L = 0.44$. The model tip deflections for a Mach number of 0.78 are shown in figure 4. Airfoil coordinates for the winglets are presented in table I.

Boundary-layer transition strips.- Boundary-layer transition strips were placed at the 5-percent-chord line on the upper and lower surfaces of the wing, at the 5-percent-chord line on the upper surface of the winglets, and at the 35-percent-chord line on the lower surface of the winglets. These strips were comprised of a 0.15-cm-wide (0.06-in.) band of carborundum grains set in a plastic adhesive. The carborundum grains were sized on the basis of reference 12. The transition strips on the lower surface of the winglets were located rearward in an attempt to simulate full-scale Reynolds number boundary-layer conditions (ref. 13). The strips on the upper surface of the winglets were located forward to insure transition ahead of the shock wave for the various test conditions.

Test conditions.- Experimental data are presented for the design Mach number of 0.78 only. For this Mach number the tests were conducted at a dynamic pressure of 41 kN/m^2 (850 psf) which resulted in a Reynolds number of 17.2×10^6 per meter (5.25×10^6 per foot).

Measurements.- Force and moment data were obtained with a five-component electrical strain-gage balance. Side-force measurements were not taken. The angle of attack was measured with a device located within the fuselage.

Chordwise static-pressure distributions were measured at four spanwise stations on the wing. In addition, they were measured at three stations on the upper winglet and one on the lower for the configurations with the winglets.

Results and Discussion

Results.- The variations of drag coefficient, pitching-moment coefficient, and angle of attack with lift coefficient at the design Mach number of 0.78 are presented in figure 5 for the basic wing and for configurations with the upper winglet, upper and lower winglets, and a wing-tip extension. The increase in lift coefficient for a constant drag coefficient resulting from the additional surfaces is presented in figure 6. These changes are equivalent to changes in the lift-drag ratio. The effects presented differ from those for a complete full-scale airplane. At full-scale conditions the skin friction drag penalties associated with the additions would be somewhat less than those for the test Reynolds number. More importantly, the drag due to lift for the complete airplane would be greater than for the exposed panel of the wind-tunnel configuration. Therefore, the relative increase in lift coefficient for a constant drag coefficient would be less. It has been estimated that because of these two compensating factors the relative changes for the total full-scale airplane would be about 10 percent less than those shown in figure 6.

The increase in bending-moment coefficient (at a constant lift coefficient) at the horizontal elastic axis of the wing-fuselage juncture resulting from the additional surfaces is presented in figure 7. The values shown were obtained by correcting the rolling-moment increments measured by the balance for the moments determined by multiplying the side-force increments by the vertical distance from the balance center to the elastic axis of the wing root. These side-force increments, not measured by the balance, were obtained by integrating the measured pressure distributions on the wing and winglets.

Span load distributions for the design Mach number and near the design lift coefficient are presented in figure 8 for the various configurations. Selected pressure distributions for the same conditions are presented in figure 9. The ratio of the normal-force coefficient for the upper winglet to the lift coefficient for the total configuration is presented in figure 10.

10

The effect of changing the incidence of the upper winglet on the drag for the configuration with both the upper and the lower winglets is shown in figure 11. The effects of these incidence changes on the span load distributions are shown in figure 12.

Effect of upper winglet only.- Addition of the upper winglet only increases the lift-drag ratio of the exposed wing panel by about 9 percent near design conditions of $M_\infty = 0.78$ and $C_{L,\text{basic wing}} = 0.44$ (fig. 6). At higher lift coefficients the improvement is decreased because of wave drag and boundary-layer separation associated with a strong shock wave in the region of the juncture of the winglet and wing tip. Unpublished results indicate that at lower Mach numbers the losses in winglet effectiveness at higher lift coefficients are much less severe.

An analysis of the results of figure 5 indicates that addition of the upper winglet reduces the basic induced drag by about 20 percent for lift coefficients up to the design value. This reduction is substantially greater than the value predicted in reference 3 for a vertical tip mounted surface with the same ratio of height to wing span as the winglet investigated. Calculations based on the theories of references 7 and 9 indicate that the difference is due primarily to the tilt of the winglet outward. Calculations based on reference 9 indicate that the dihedral and bending of the wing investigated also slightly increase the effectiveness of the winglet.

Reductions in induced drag obtained in this investigation are associated with an approximately elliptical span load distribution on the basic wing (fig. 8). Calculations based on reference 9 indicate that the reductions would be significantly less for a wing with the center of lift located further inboard.

Adding the upper winglet results in somewhat more negative pitching-moment coefficients (fig. 5). An analysis, based on the aerodynamic characteristics for the complete airplane, indicates that these changes in pitching-moment coefficient would have only a slight effect on the trim drag for the airplane. With the winglet added the breaks in the variations of angle of attack and pitching-moment coefficient with lift coefficient occur at approximately the same lift coefficient but are slightly more severe.

As indicated in the section "Design Considerations," the loads on the upper winglet and the added loads on the outboard region of the wing associated with adding the upper winglet, shown in figure 8, are substantially less than the theoretical values for minimum induced drag determined by the theories of references 3, 7, and 9. For the configuration of this investigation the measured loads on the winglet are about two-thirds of the optimum theoretical values and the added loads on the wing are about one-half of the optimum theoretical values. For other wing configurations, these ratios may be somewhat different.

At lift coefficients from the design value to the value at which the angle-of-attack and pitching-moment-coefficient curves break (approximately 0.7), the normal-force coefficient for the winglet is roughly the same as the lift coefficient (fig. 10). The decrease

in the relative magnitude of winglet normal-force coefficient at higher lift coefficients is associated with the unloading of the outboard region of the wing due to increased boundary-layer separation on the wing at these conditions.

Effect of adding lower winglet.- Near design conditions of $M_\infty = 0.78$ and $C_{L,basic\ wing} = 0.44$, adding the lower winglet has little effect on the lift-drag ratio (fig. 6). However, at higher lift coefficients, adding the lower winglet results in a significant improvement in the lift-drag ratio (fig. 6). As indicated in the section "Design Considerations," these favorable effects of adding the lower winglet for higher lift coefficients are associated with reductions in the relatively high induced velocities on the forward region of the inner surface of the winglet and near the tip region of the wing opposite the forward part of the upper winglet (fig. 9) with consequent reduction in shock-induced boundary-layer separation.

Adding the lower winglet also reduces the severity of breaks in the angle-of-attack and pitching-moment-coefficient curves (fig. 5). With this surface added the severity of the break is about the same as for the wing alone.

Adding this surface increases the loads on the outboard region of the wing (fig. 8) with a resulting increase in the bending-moment increments at the wing-fuselage juncture (fig. 7). Data obtained at the one row of pressure orifices on the lower winglet indicate that, as for the upper winglet, the normal-force coefficients on the lower winglet are about the same as the lift coefficients for the wing near design conditions.

An analysis of the effects of adding the lower winglet for all flight conditions indicates that the improvement in overall performance would be marginal. Modification of this surface, as suggested in the section "Design Considerations," may change this conclusion.

Effect of upper winglet incidence.- Near design conditions of $M_\infty = 0.78$ and $C_L = 0.48$ for the configuration with winglets, increasing the incidence of the upper winglet above -4° (selected for the final configuration) increases the drag coefficient (fig. 11). This incidence increase also significantly increases the loads on both the winglet and the outboard region of the wing (fig. 12) with a resulting increase in bending moments imposed on the structure.

Comparison with tip extension.- The tip extension investigated has a span equal to 0.38h. The added wing area is about 90 percent of the exposed surface area of the upper winglet. The increase in root bending moment for the tip extension is approximately the same as the increase for the upper and lower winglets, and it is greater than the increase for the upper winglet only (fig. 7). Near design conditions of $M_\infty = 0.78$ and $C_{L,basic\ wing} = 0.44$, this extension increases the lift-drag ratio by about 4 percent (fig. 6) which is less than half that achieved by adding the winglets.

12

Calculations of local bending moments along the span of the wing based on the span load distributions (similar to those presented in ref. 4) indicate that adding the winglets increases the bending moments on the outboard region of the wing by somewhat greater amounts than does the tip extension selected. Studies made by industry have indicated that such bending-moment differences usually have relatively small effects on the wing structural weight.

The increase in lift coefficient for a given angle of attack associated with adding the tip extension is about the same as that for the winglets. However, the increase in negative pitching-moment coefficient associated with adding the tip extension is somewhat greater than that for the winglets (fig. 5). With the tip extension the positive break in the variation of pitching-moment coefficient with lift coefficient occurs at the same lift coefficient and has about the same magnitude as the break for the basic wing and for the configuration with the upper and lower winglets.

CONCLUDING REMARKS

A wind-tunnel investigation at high subsonic speeds of winglets mounted on the tip of a first-generation, narrow-body jet transport wing has been conducted. The winglets, designed on the basis of the approach presented herein, are compared with a wing-tip extension producing the same increase in bending moment at the wing-fuselage juncture as do the winglets. Selected results are presented and indicate the following:

1. At the design Mach number of 0.78 and near the design wing lift coefficient of about 0.44, adding the winglets reduces the induced drag by about 20 percent and increases the wing lift-drag ratio by approximately 9 percent. This improvement in lift-drag ratio is more than twice as great as that achieved by the wing-tip extension.

2. The negative increments in the pitching-moment coefficient associated with adding the winglets are less than those produced by the wing-tip extension.

3. The normal-force coefficients for the winglets are about the same as the lift coefficient for the wing near design conditions.

4. The magnitude of the increase in overall performance improvement provided by addition of the winglets in comparison with that for the wing-tip extension is significantly dependent on the angles of incidence of the upper winglet and the associated loads on this winglet and on the outboard region of the wing. The greatest measured improvement in overall performance is obtained with substantially smaller loads than those calculated for minimum induced drag by available theory.

5. An analysis of the effects at all flight conditions of an auxiliary winglet below the wing tip indicates that the improvement in overall performance would be marginal.

Langley Research Center
National Aeronautics and Space Administration
Hampton, Va. 23665
June 10, 1976

REFERENCES

1. Nagel, F.: Wings With End Plates. Memo. Rep. 130, Eng. Div., McCook Field, Nov. 4, 1924.

2. Mangler, W.: The Lift Distribution of Wings With End Plates. NACA TM 856, 1938.

3. Weber, J.: Theoretical Load Distribution on a Wing With Vertical Plates. R. & M. No. 2960, British A.R.C., 1956.

4. Flechner, Stuart G.; Jacobs, Peter F.; and Whitcomb, Richard T.: A High Subsonic Speed Wind-Tunnel Investigation of Winglets on a Representative Second-Generation Jet Transport Wing. NASA TN D-8264, 1976.

5. Bower, Robert E.: Opportunities for Aerodynamic-Drag Reduction. NASA/University Conference on Aeronautics. NASA SP-372, 1975, pp. 323-352.

6. Mechtly, E. A.: The International System of Units — Physical Constants and Conversion Factors (Second Revision). NASA SP-7012, 1973.

7. Lundry, J. L.: A Numerical Solution for the Minimum Induced Drag, and the Corresponding Loading, of Nonplanar Wings. NASA CR-1218, 1968.

8. Lamar, John E.: A Vortex-Lattice Method for the Mean Camber Shapes of Trimmed Noncoplanar Planforms With Minimum Vortex Drag. NASA TN D-8090, 1976.

9. Goldhammer, M. I.: A Lifting Surface Theory for the Analysis of Nonplanar Lifting Systems. AIAA Paper No. 76-16, Jan. 1976.

10. McGhee, Robert J.; Beasley William D.; and Somers, Dan M.: Low-Speed Aerodynamic Characteristics of a 13-Percent-Thick Airfoil Section Designed for General Aviation Applications. NASA TM X-72697, 1975.

11. Schaefer, William T., Jr.: Characteristics of Major Active Wind Tunnels at the Langley Research Center. NASA TM X-1130, 1965.

12. Braslow, Albert L.; and Knox, Eugene C.: Simplified Method for Determination of Critical Height of Distributed Roughness Particles for Boundary-Layer Transition at Mach Numbers From 0 to 5. NACA TN 4363, 1958.

13. Blackwell, James A., Jr.: Preliminary Study of Effects of Reynolds Number and Boundary-Layer Transition Location on Shock-Induced Separation. NASA TN D-5003, 1969.

TABLE I.- AIRFOIL COORDINATES FOR WINGLETS

x/c	z/c for —	
	Upper surface	Lower surface
0	0	0
.0020	.0077	-.0032
.0050	.0119	-.0041
.0125	.0179	-.0060
.0250	.0249	-.0077
.0375	.0296	-.0090
.0500	.0333	-.0100
.0750	.0389	-.0118
.1000	.0433	-.0132
.1250	.0469	-.0144
.1500	.0499	-.0154
.1750	.0525	-.0161
.2000	.0547	-.0167
.2500	.0581	-.0175
.3000	.0605	-.0176
.3500	.0621	-.0174
.4000	.0628	-.0168
.4500	.0627	-.0158
.5000	.0618	-.0144
.5500	.0599	-.0122
.5750	.0587	-.0106
.6000	.0572	-.0090
.6250	.0554	-.0071
.6500	.0533	-.0052
.6750	.0508	-.0033
.7000	.0481	-.0015
.7250	.0451	.0004
.7500	.0419	.0020
.7750	.0384	.0036
.8000	.0349	.0049
.8250	.0311	.0060
.8500	.0270	.0065
.8750	.0228	.0064
.9000	.0184	.0059
.9250	.0138	.0045
.9500	.0089	.0021
.9750	.0038	-.0013
1.0000	-.0020	-.0067
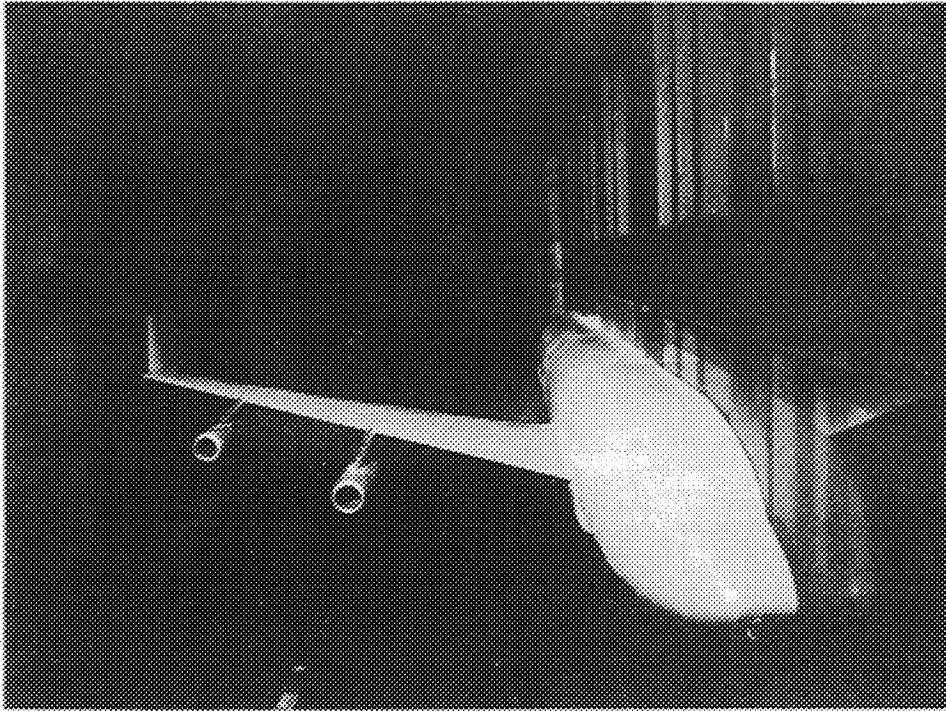
L-75-8430

(a) Complete configuration.
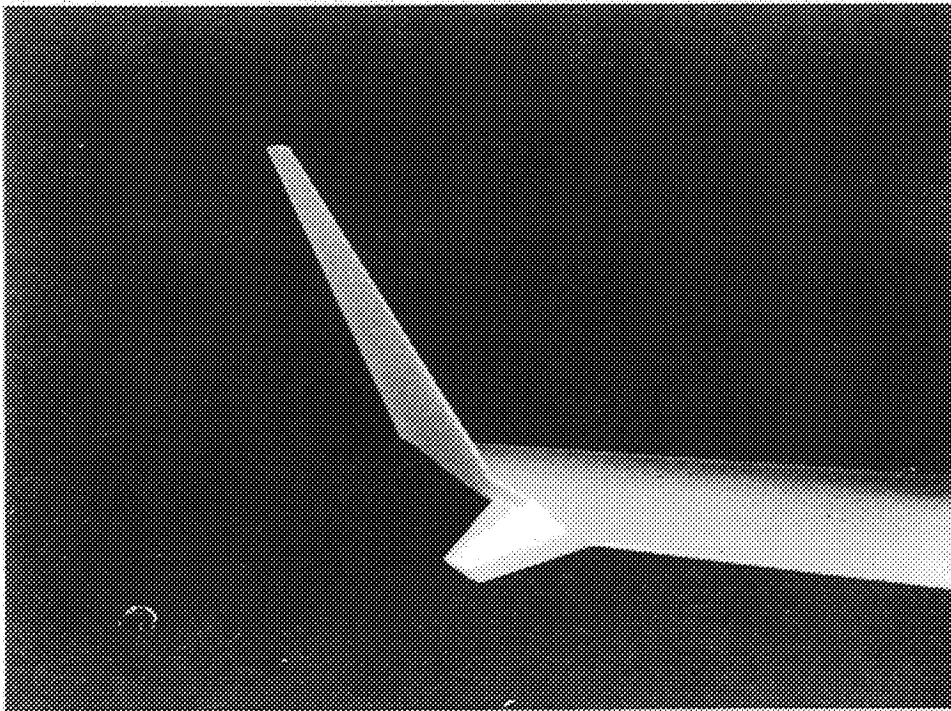
L-75-8429

(b) Winglets.

Figure 1.- Wind-tunnel model.
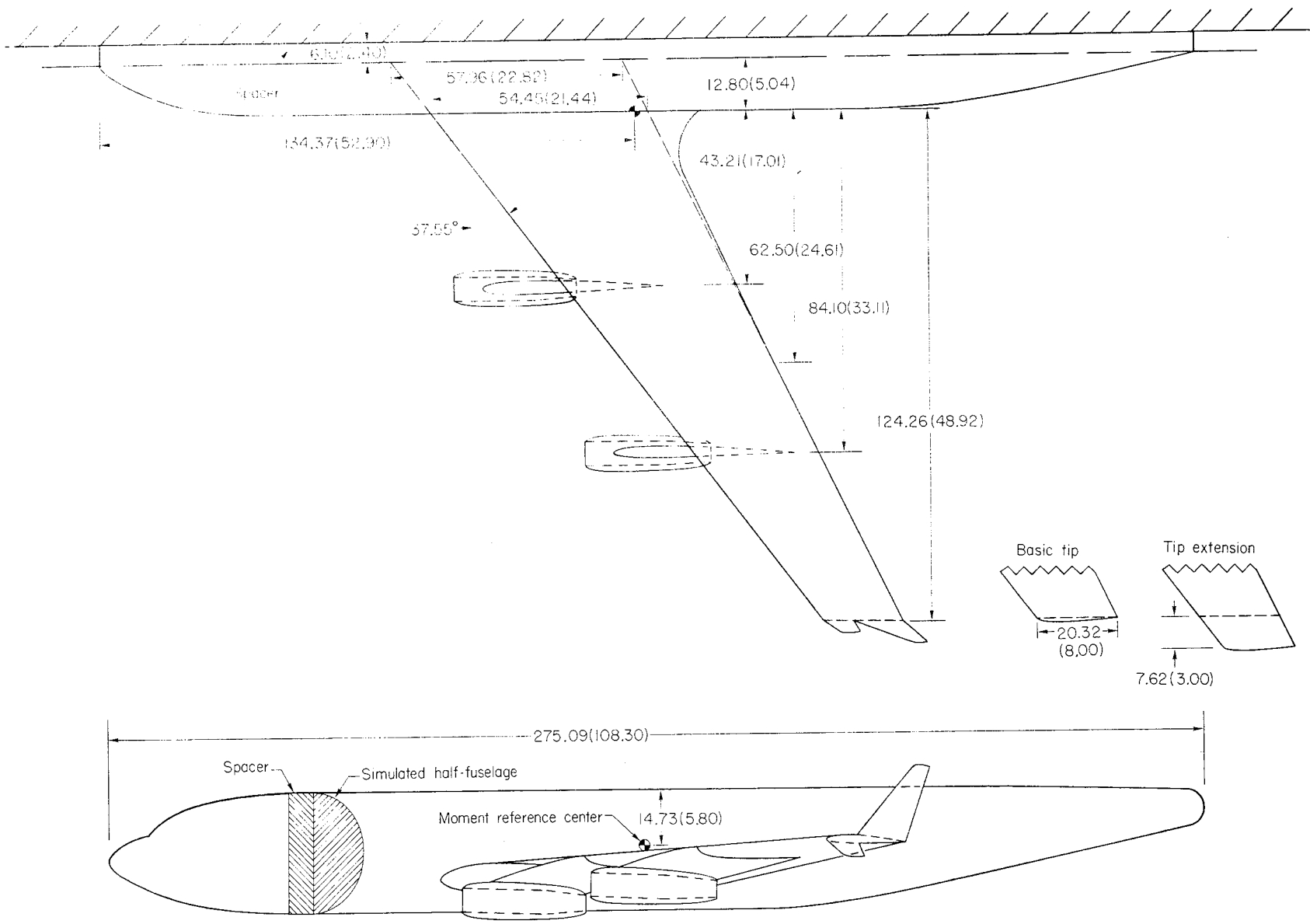
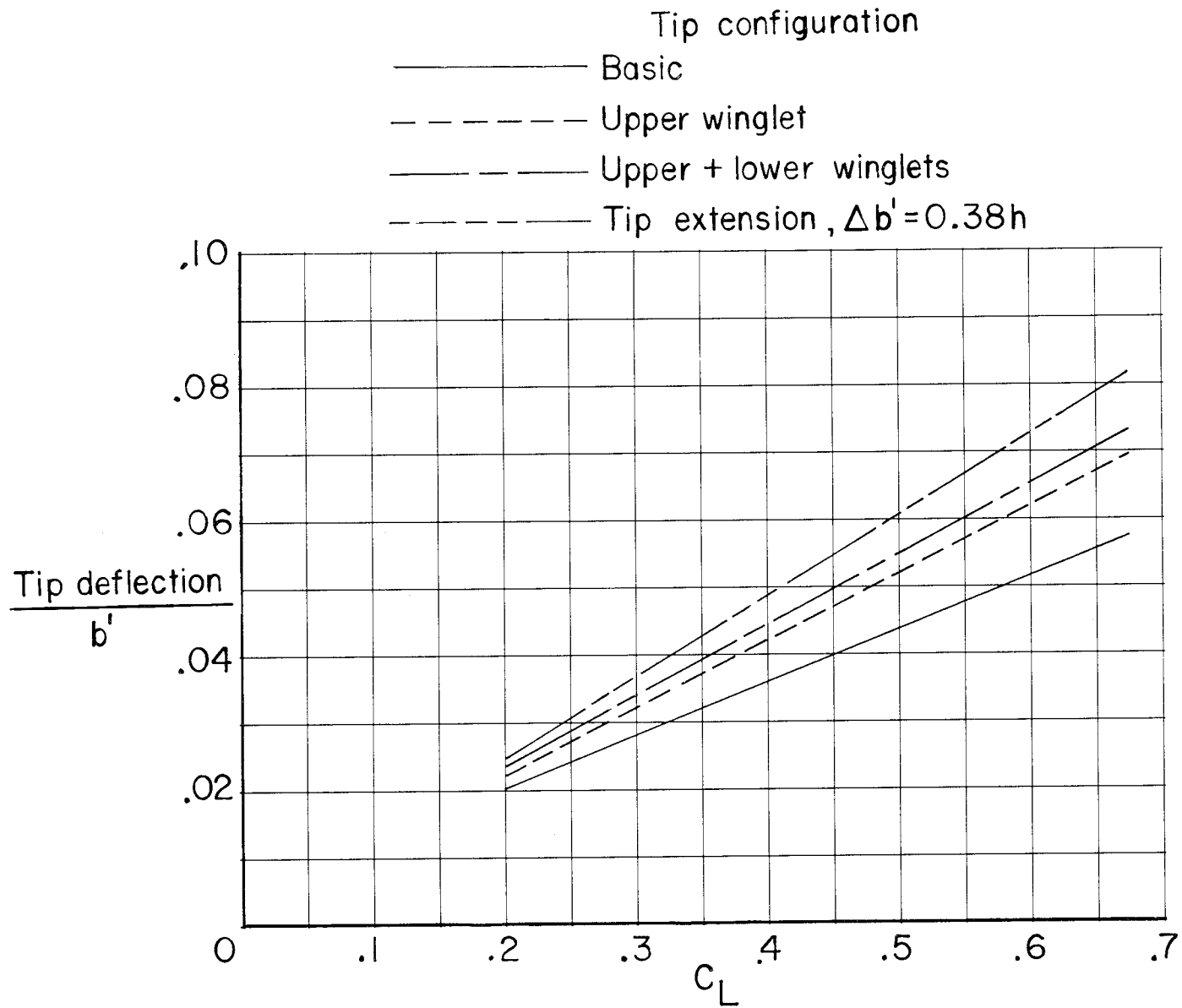Figure 2.- Drawing of semispan model. Dimensions are in centimeters (inches).

Typical winglet section

Upper surface

$-i$

| Winglet	i, deg
Upper	-4
Lower, root	-7
Lower, tip	-11

Section A—A

$.21c_t$

Span, $h = c_t$

$38°$

$.65c_t$

$.40c_t$

Span $= 0.23c_t$

$52°$

$.16c_t$

c_t

Upper surface

$15°$

Dihedral

$7°$

Upper surface

$36°$

A

A

Figure 3.- Winglets.

Tip configuration
——————— Basic
— — — — — — Upper winglet
——— — ——— Upper + lower winglets
— —— — ——— Tip extension, $\Delta b' = 0.38h$
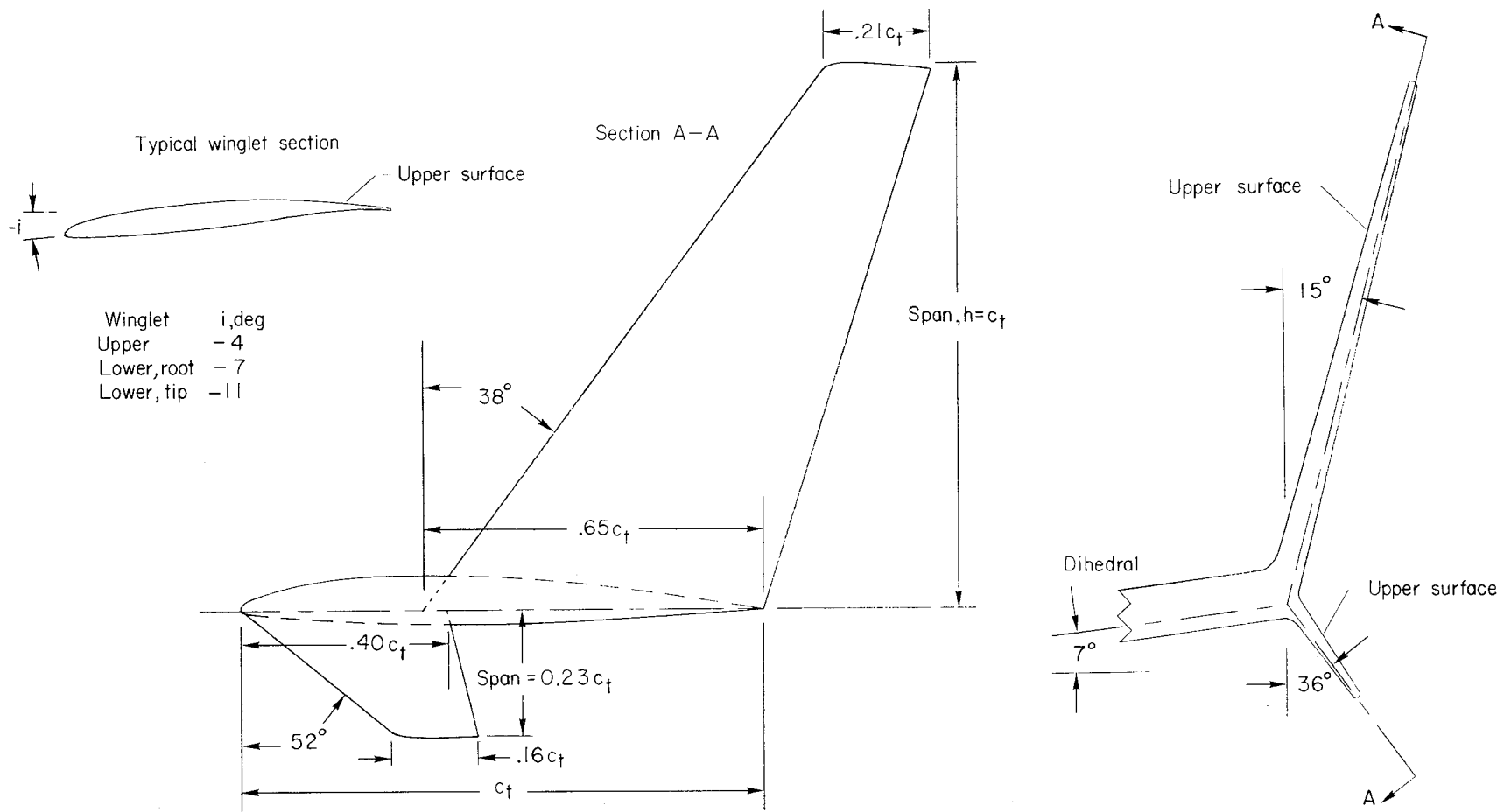
Figure 4.- Wing-tip deflections. $M_\infty = 0.78$.
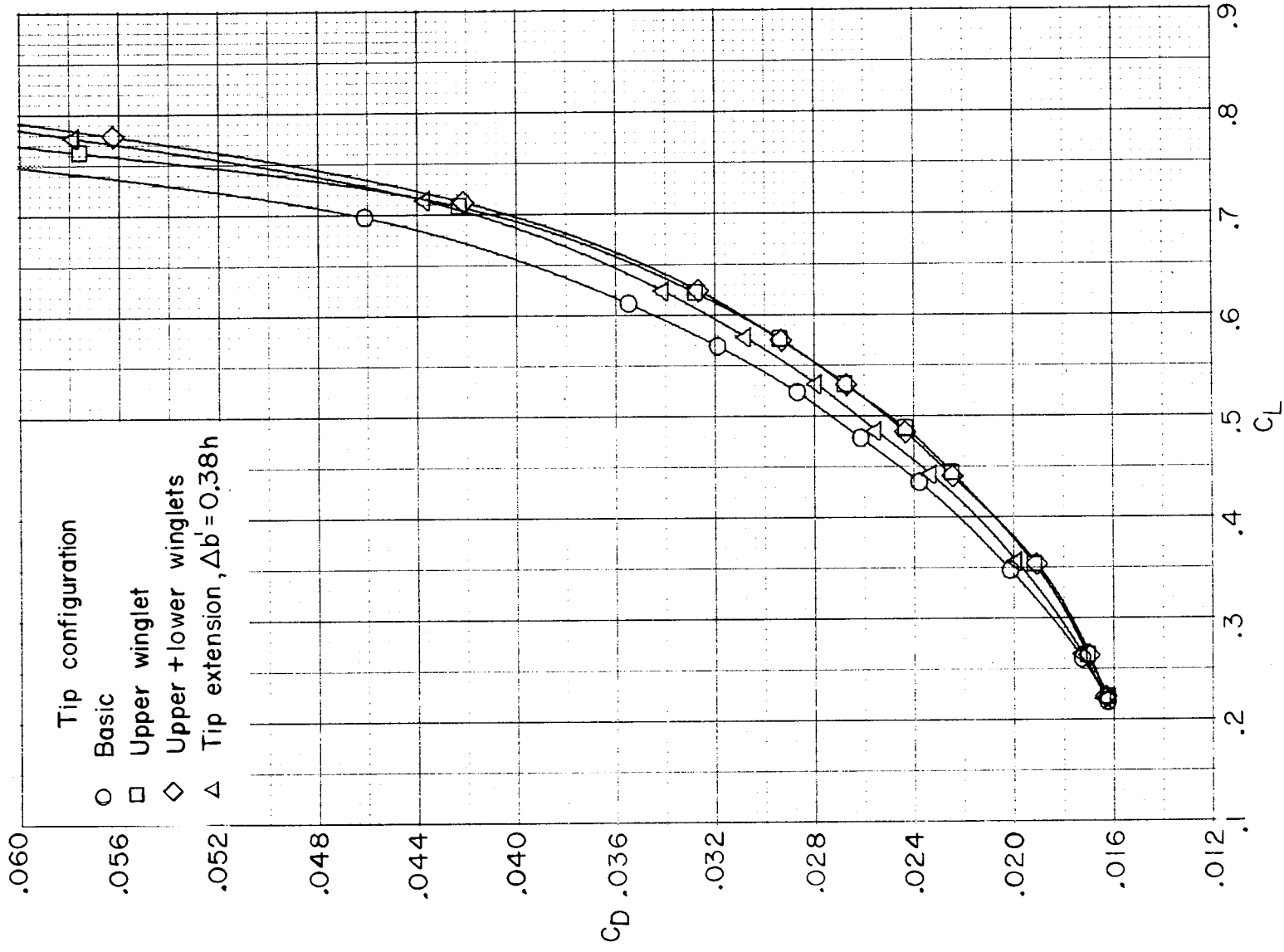
(a) Drag.

Figure 5.- Variations of drag coefficient, angle of attack, and pitching-moment coefficient with lift coefficient. $M_\infty = 0.78$.
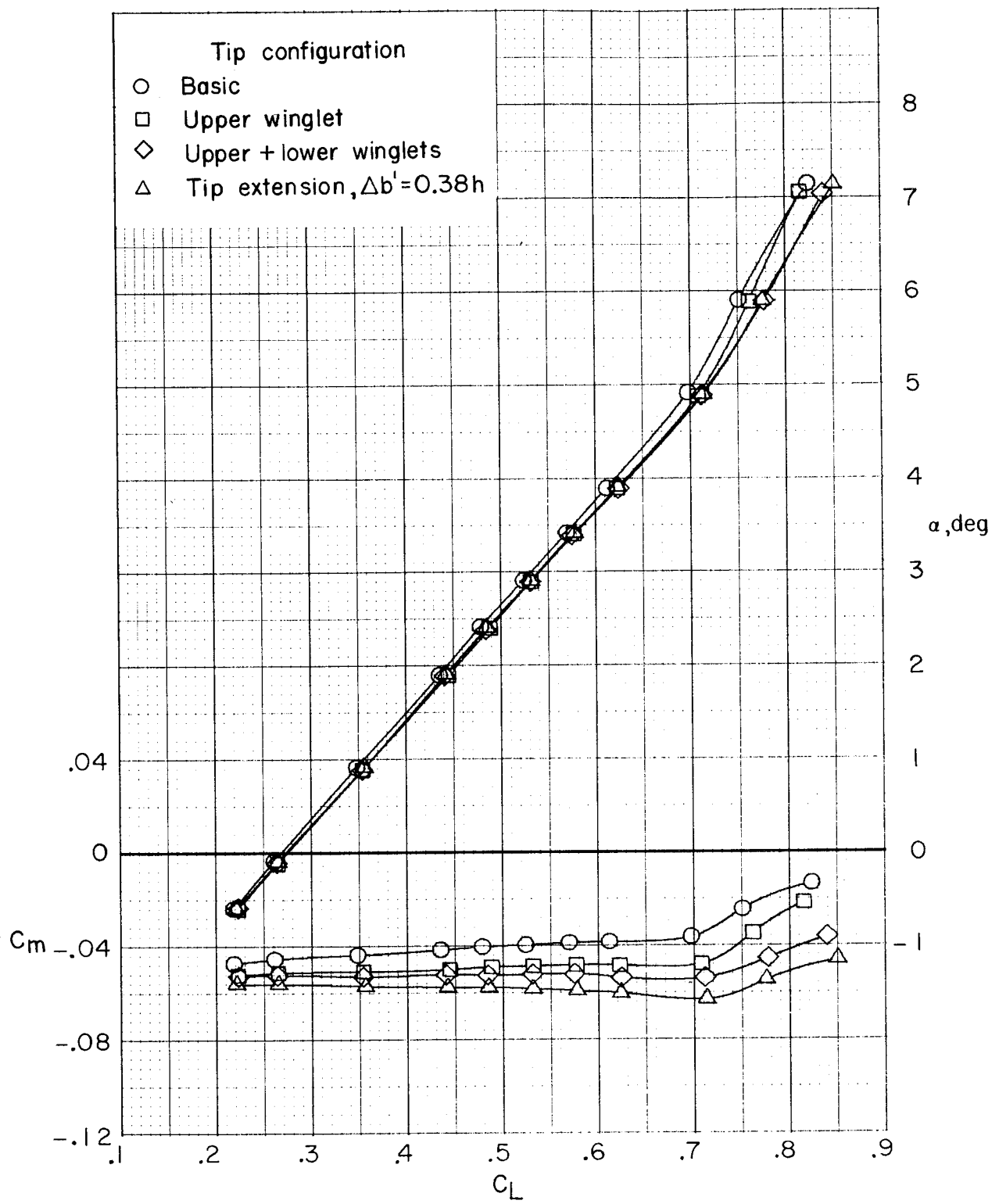
(b) Angle of attack and pitching moment.

Figure 5.- Concluded.

Tip configuration

————————— Upper winglet

— — — — — Upper + lower winglets

——— — — Tip extension, $\Delta b' = 0.38h$
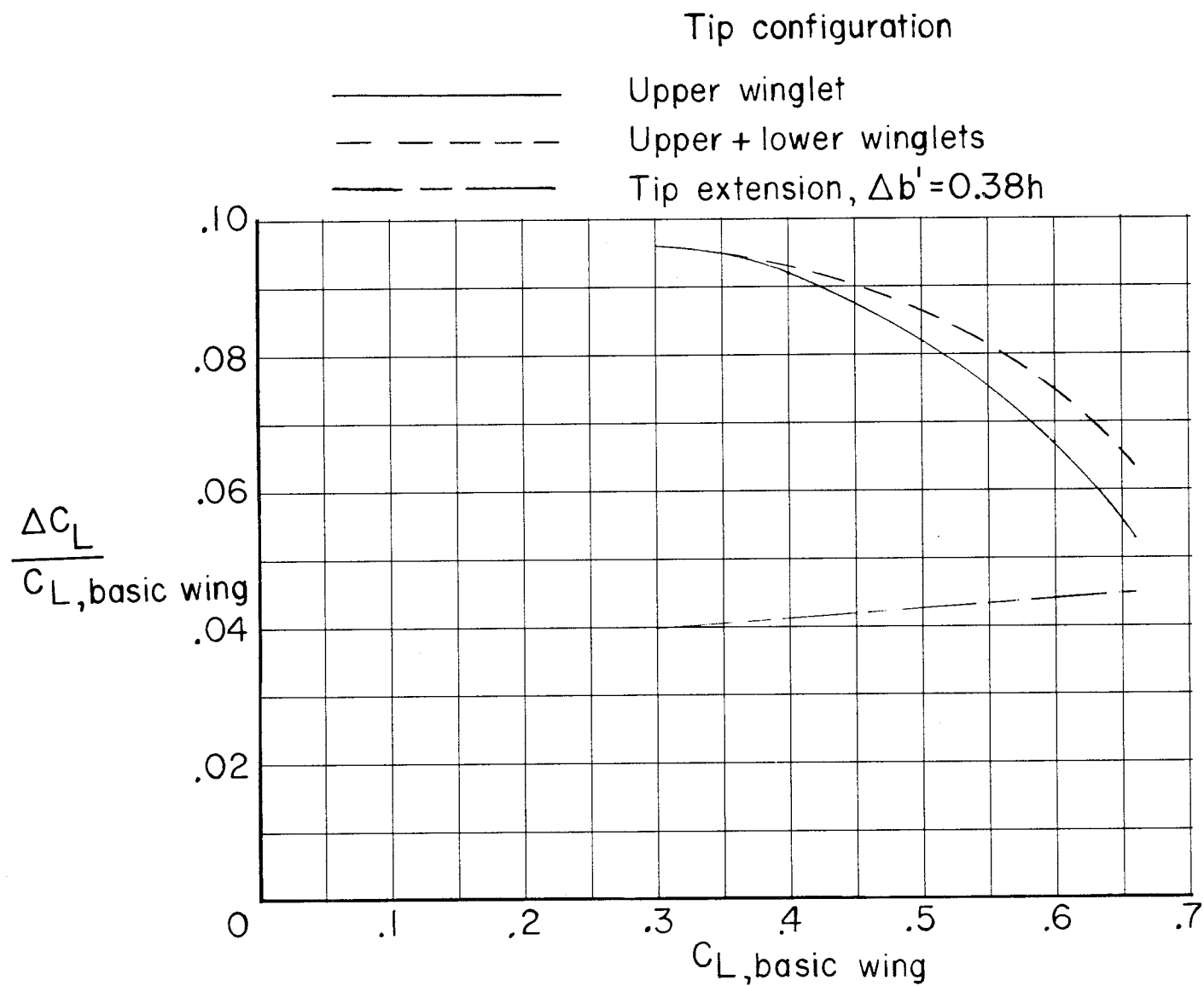
Figure 6.- Variation of incremental lift coefficient for constant drag coefficient with lift coefficient. $M_\infty = 0.78$.
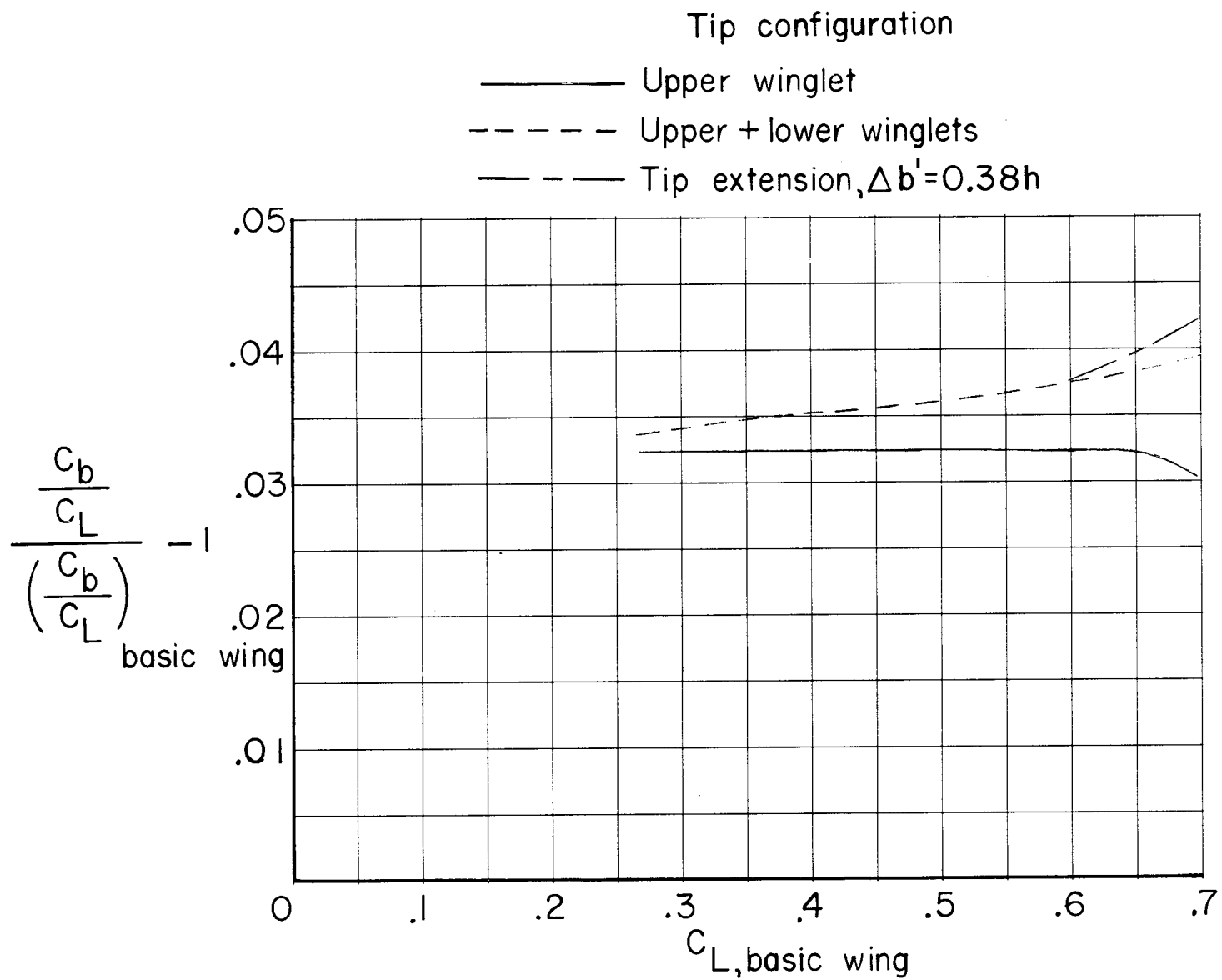
Figure 7.- Variation of incremental bending-moment coefficient at wing-fuselage juncture with lift coefficient. $M_\infty = 0.78$.
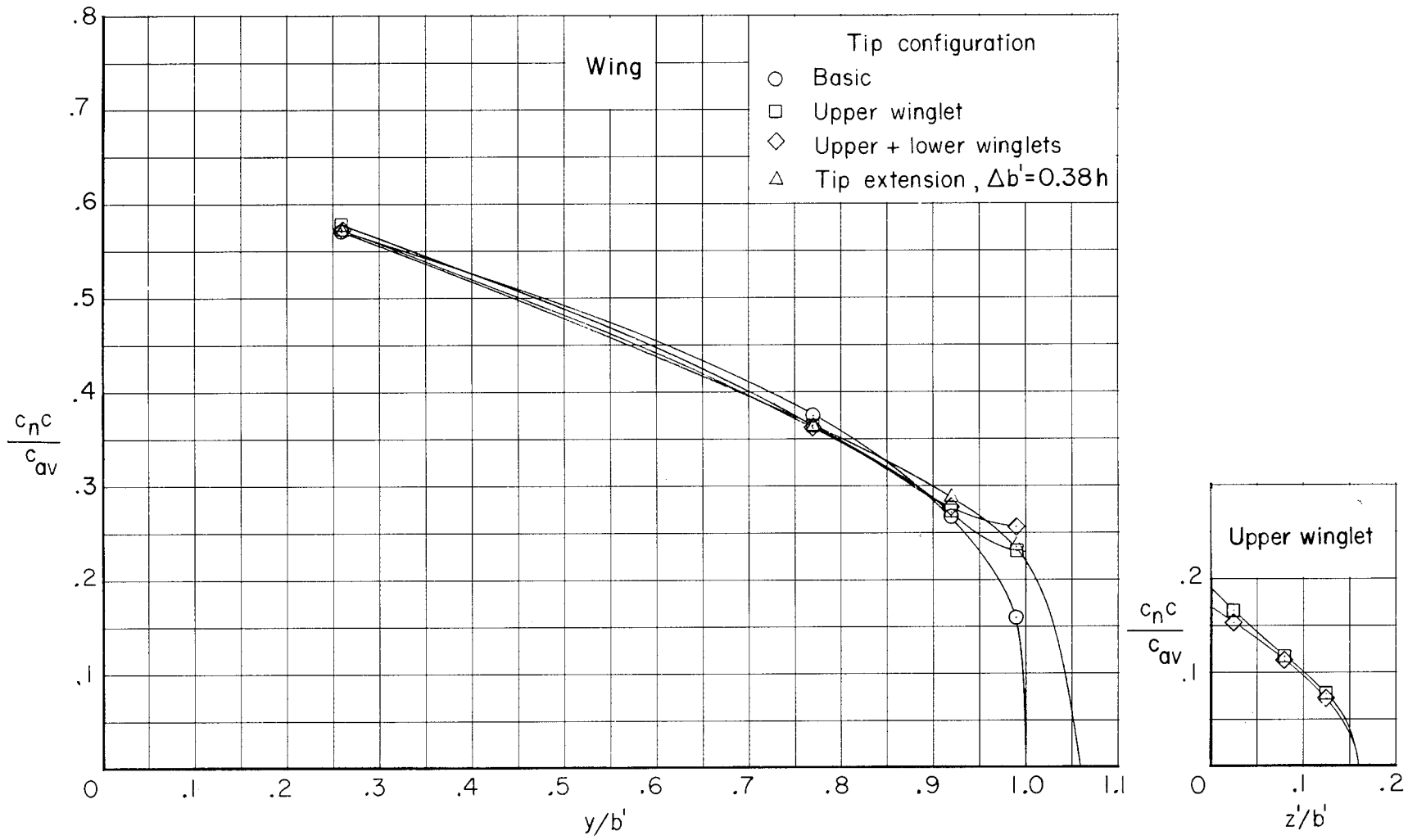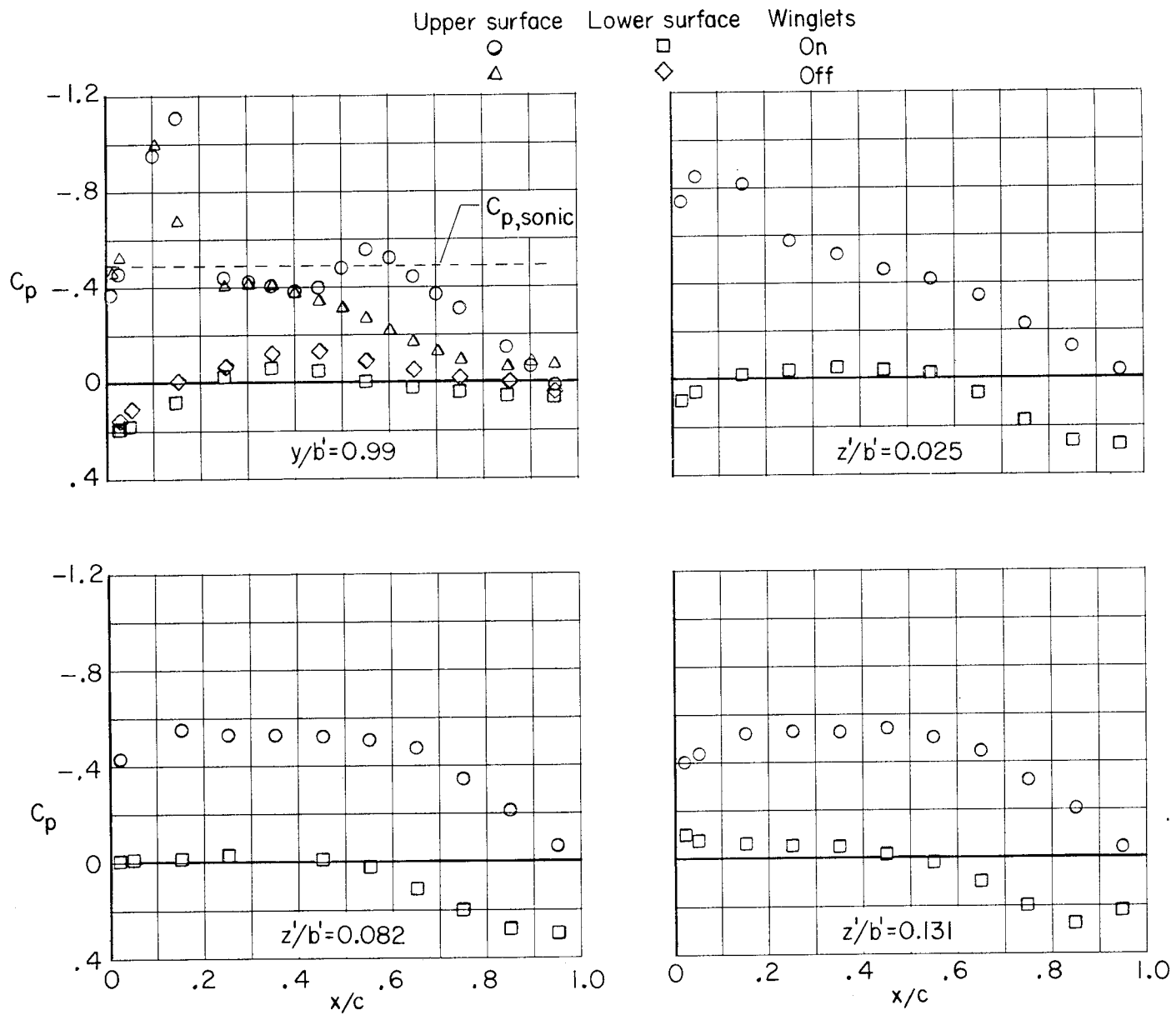
Figure 8.- Span load distributions. $M_\infty = 0.78$; $C_L \approx 0.48$.

Upper surface   Lower surface   Winglet
○   □   On
△   ◇   Off
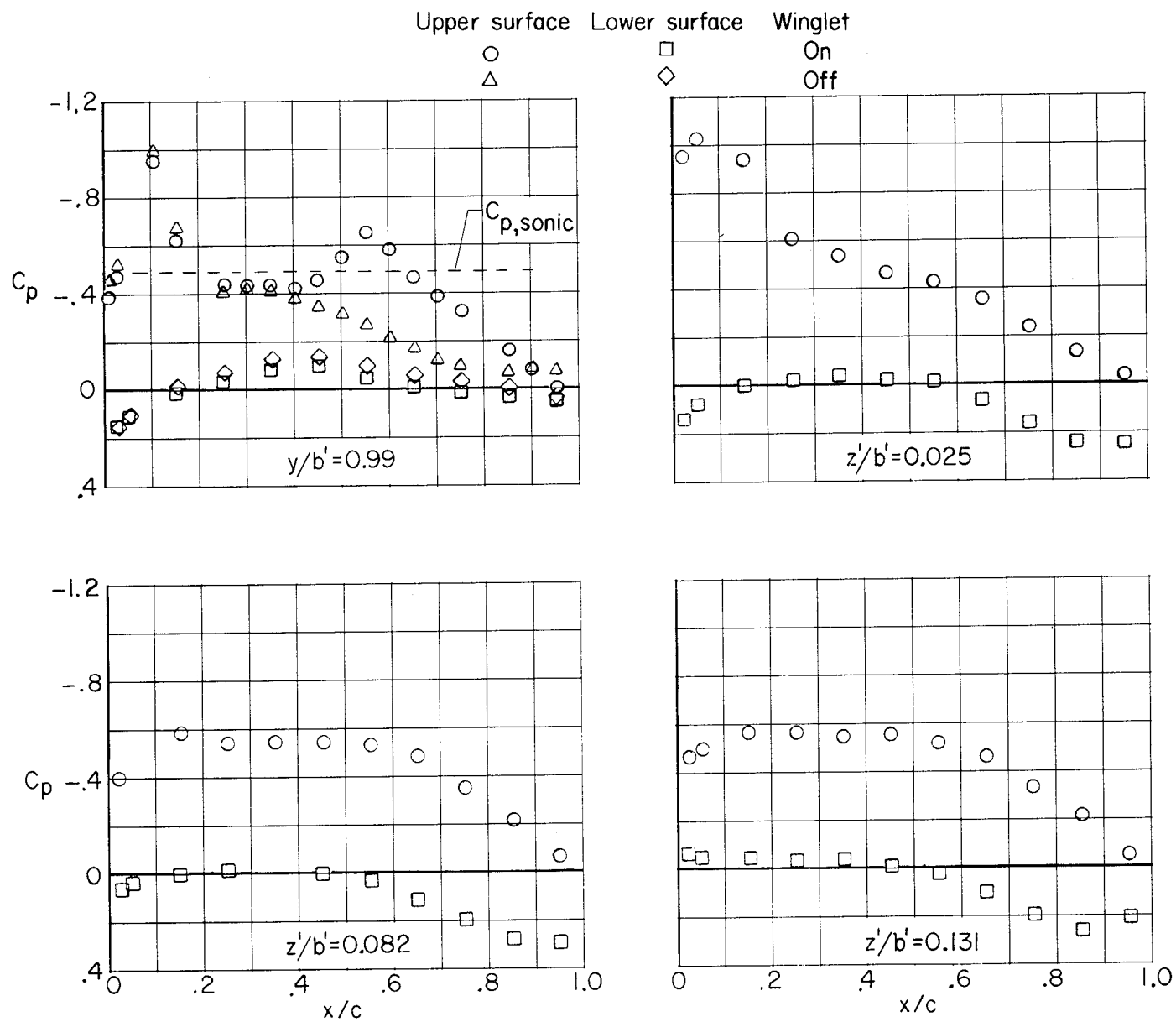
(a) Configuration with upper winglet.

Figure 9.- Chordwise pressure distributions. $M_\infty = 0.78$; $C_L \approx 0.48$.

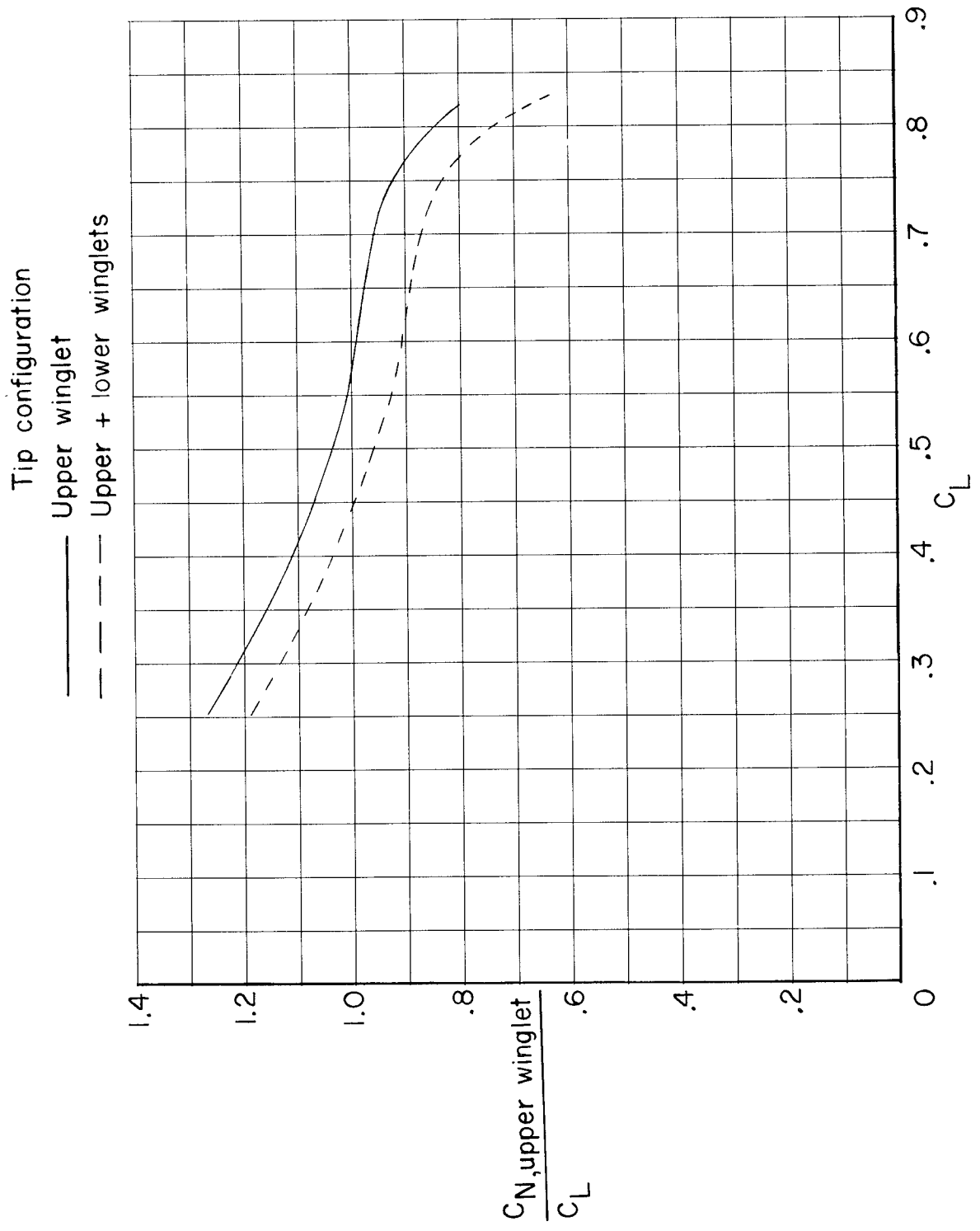(b) Configuration with upper and lower winglets.

Figure 9.- Concluded.

Figure 10.- Variation of ratio of normal-force coefficient for the upper winglet to lift coefficient for total configuration with lift coefficient. $M_\infty = 0.78$.
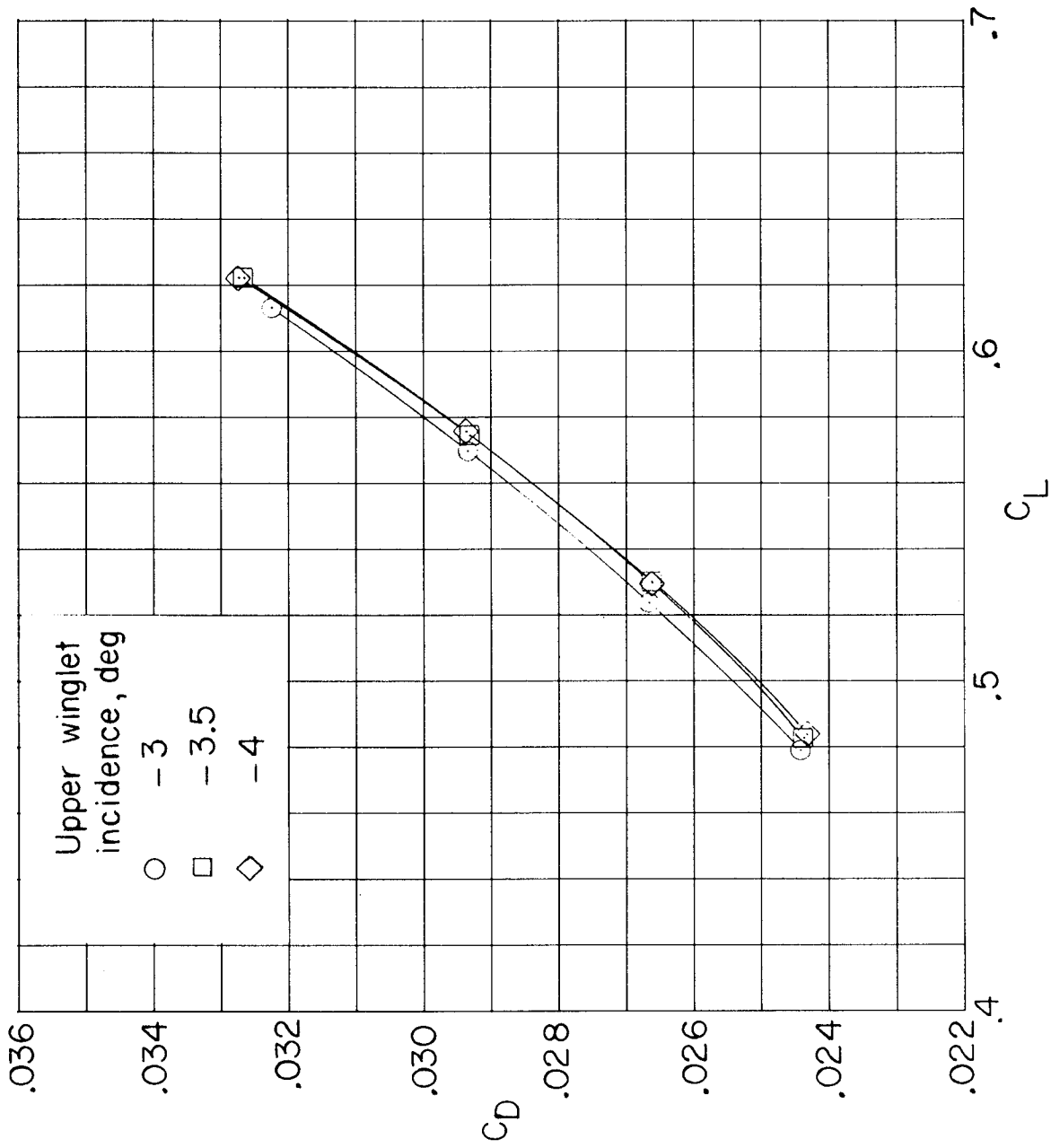
Figure 11.- Effect of angle of incidence of upper winglet on variation of drag coefficient with lift coefficient for configuration with both upper and lower winglets. $M_\infty = 0.78$.
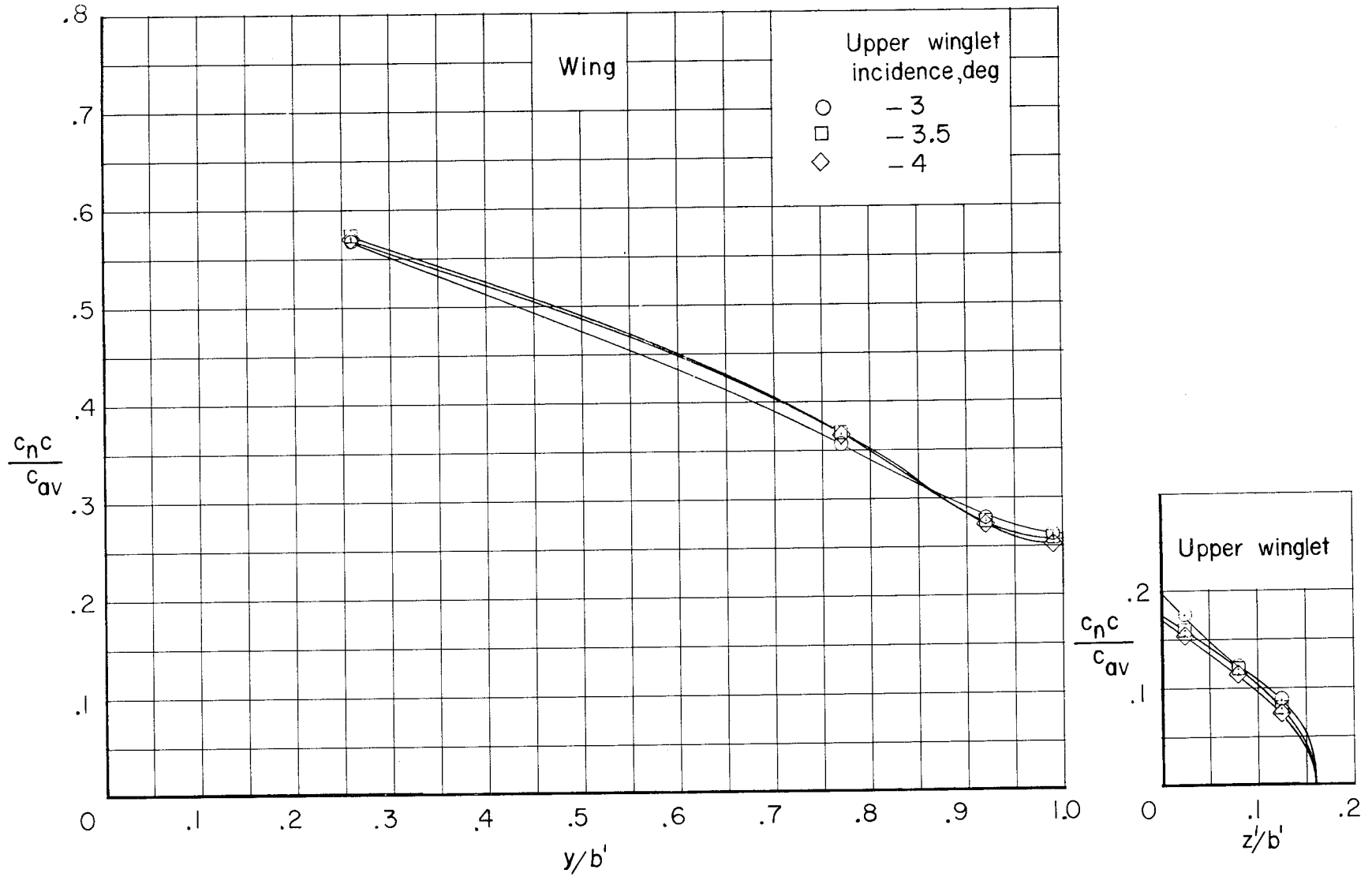
Figure 12.- Effect of angle of incidence of upper winglet on span load distributions for configuration with both upper and lower winglets. $M_\infty = 0.78$.